Simulating growth dynamics of filamentous fungal biofilms

Thesis

Submitted in partial fulfillment of the requirements of

BITS F422T

BY

Ankush G K
2017B5A41552H

Under the supervision of

Prof. Aravinda N. Raghavan
Associate Professor
BITS Pilani Hyderabad Campus

BITS Pilani
Hyderabad Campus

BIRLA INSTITUTE OF TECHNOLOGY AND SCIENCE, PILANI
HYDERABAD CAMPUS
(May, 2022)

Abstract

Biofilms are fascinating structures built by microorganisms almost everywhere. They can be found in wide range of places: from wounds to river beds to extreme environments. Biofilms have been instrumental in treatment of polluted environments while on the other hand, they are a dangerous entity causing numerous health concerns. This dual nature calls for a need to understand the workings of the biofilm, how they form, what affects them etc. Different species of microorganisms like bacteria, fungi or protozoa form different kinds of biofilms. Common features of all biofilms: biofilm matrix and its components, the stages of formation, etc. are also covered. Focus is given on filamentous fungal biofilm. These biofilms show branching patterns during growth and in the end a network of filaments (hyphae) is formed. Their growth process is discussed. A good test of our understanding of the processes is to mathematically model them. A continuum model with system of five coupled partial differential equations is introduced which models the filamentous fungal growth. Every process from the intake of nutrients to the branching of filaments is modelled. Simulations of a single inoculation site and its results are discussed via several plots. The mechanism of distribution of nutrients inside a hyphae (*translocation*) is found to be of two types: Passive and Active. The roles played by each of them and how they affect the growth of the biofilm with changes in the growth conditions are also covered. In experiments carried out in [1], the inoculum is distributed all over the domain. To mimic that to an extent, multiple inoculation sites were simulated and analysed. This thesis covers only simulation of the growth of the biofilm in a homogeneous external substrate. Actual experimental conditions are heterogeneous and that would be worth exploring in the future.

Table of contents

1 An Overview

1.1 Why model biofilms?

There is good and bad in everything. There are good and bad biofilms too. Good biofilms are useful in sewage/waste-water treatment and decontaminating polluted areas where the microbes form a network of clusters and break down the organic material by consuming required nutrients [2](Fig. 1). Bacterial biofilms are used in food fermentation, microbial fuel cells, biofouling, prevention of corrosion etc. [3]. Bad biofilms are the leading cause of most of the health infections (for example, dental plaque, ear infections, cystic fibrosis etc.). Some biofilms show anti-microbial resistance making them difficult to deal with. Some begin to grow in the medical devices/implants (catheters, prosthesis, etc.) and affect their function [2]. Fungal biofilms have been posed as a clinical and an economic problem (Fig. 1). They are complex structures which make it difficult to diagnose and eradicate [4]. These make it important to learn about the biofilms. Understanding the inner workings of the biofilm can help us take advantage of their useful properties and tackle the dangerous ones. To bridge the gap between the experimental and theoretical understanding, modelling and simulations are extremely helpful. Another reason to model biofilms is that they are one of the oldest lifeforms and have some ingenious communication networks established at cellular level. Biofilms can be considered to be a micro-community of cells where different tasks are distributed to different cells depending on the type of species [2]. Looking at the biofilms under microscope reveals the intricate architecture of channels for transport of water or nutrients. Such complex structures built by what seem to be simple life-forms are worthy of exploration.
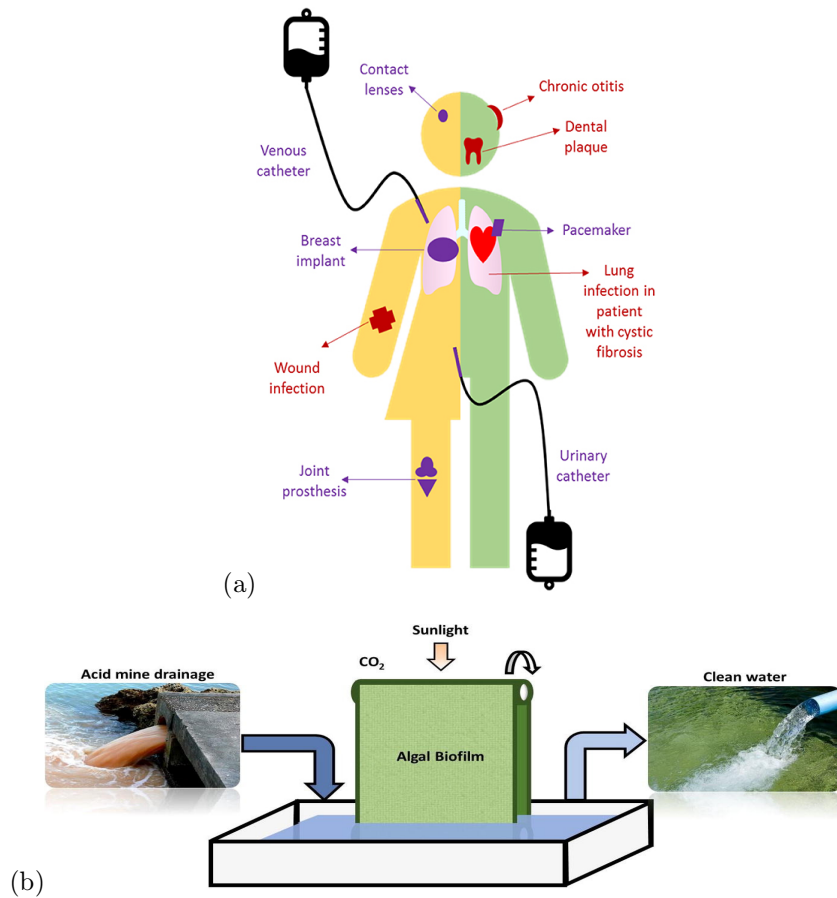

(a)

(b)

Figure 1. Top: Biofilm related infections. In red, biofilms grow on tissues, In purple biofilms grow in the implanted device. Image taken from https://www.frontiersin.org/files/Articles/505365/frym-08-00062-HTML/image_m/figure-1.jpg. Bottom: An algal biofilm reactor used to treat polluted water. Image taken from [5].

1.2 Why do microorganisms form biofilm?

It is typically assumed that the microorganisms exist individually (planktonic form). But extensive research has found that there are advantages for microorganisms to exist as a community (or biofilm). Forming a biofilm lends protection from the environment, and resistance to physical and chemical removal [4]. Microorganisms have been observed to show different properties when they exist in a biofilm as compared to when they exist individually; for example, antibiotic resistance and protection from defence mechanisms. Biofilm provides transport networks for nutrients and easy intake from the environments. The EPS secreted by the microorganisms contain some hydrophobic components which act as a skin that help combat desiccation. In other words, the quality of life in a biofilm is much better. Few more perks of biofilms are shown in Fig. 2.
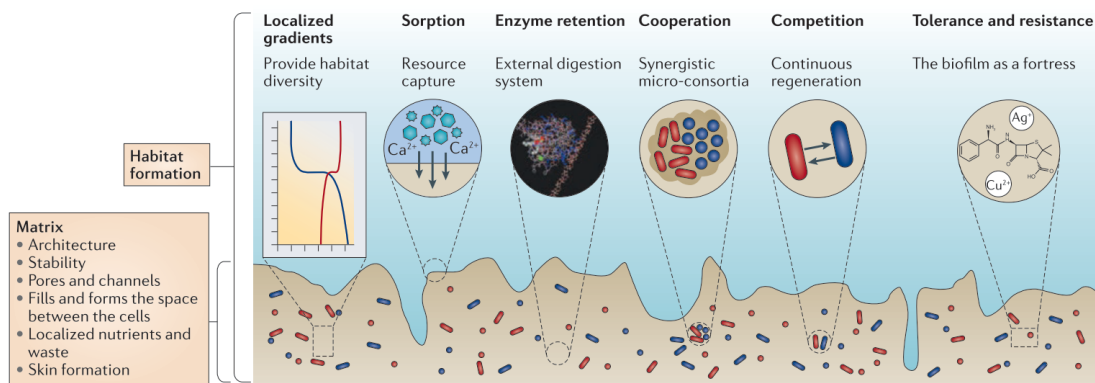

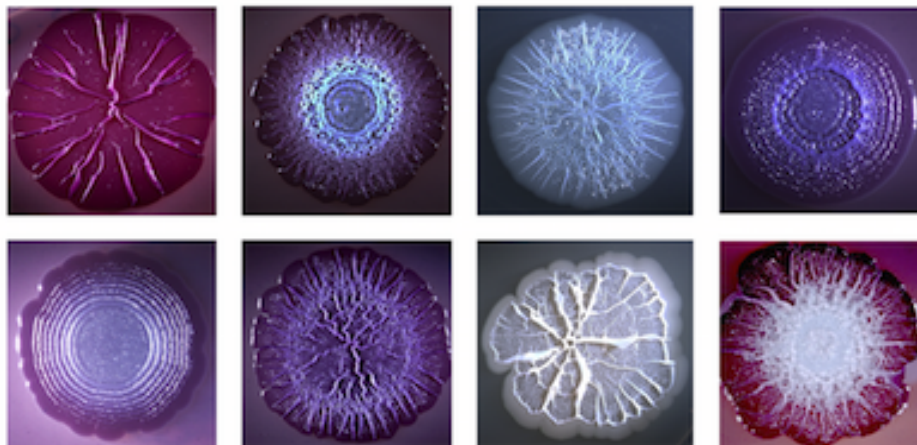**Figure 2.** Perks of being a part of biofilm. Image taken from [6]

Figure 3. Few examples of biofilms. Image taken from https://www.interdisciplinary-laboratory.hu-berlin.de/media/images/ArchitekturundMorphogenesevonBiofilmen_web.width-960.png

1.3 What are biofilms made of?

Interestingly, the microorganisms make up only 10% of dry mass of the biofilm. The remaining part is the biofilm matrix. The matrix is an assortment of various biopolymers known as Extracellular Polymeric Substances (EPS) produced by the microorganisms. The matrix keeps the microorganisms close together and provides stability and architecture to the biofilm. EPS is made up of

several components [6][7]:

- polysaccharides

- proteins

- DNA

- enzymes

- some inorganic substituents

. Each of these components have an important role to play in the community known as biofilm (Fig. 4). The largest component of the matrix is water and there are special channels/pores inside the biofilm for the transport of water. The matrix creates an environment where the water inside the biofilm does not dry quickly giving a stable water potential. For a detailed information on the role of each of the components, refer Fig. 5.
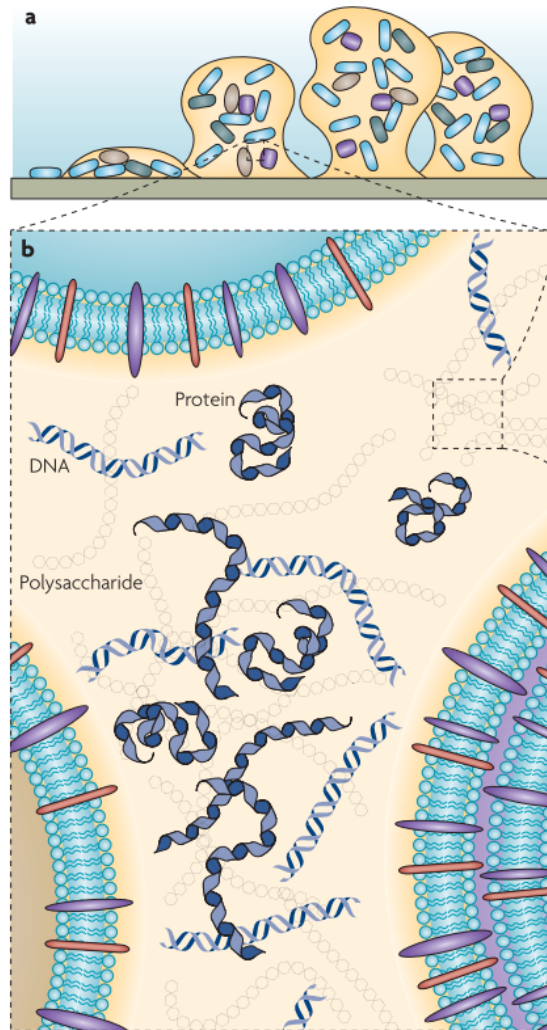

Figure 4. (a) A model of bacterial biofilm attached to a surface. (b) Major components of the matrix. Image taken from [6]

Function	Relevance for biofilms	EPS components involved
Adhesion	Allows the initial steps in the colonization of abiotic and biotic surfaces by planktonic cells, and the long-term attachment of whole biofilms to surfaces	Polysaccharides, proteins, DNA and amphiphilic molecules
Aggregation of bacterial cells	Enables bridging between cells, the temporary immobilization of bacterial populations, the development of high cell densities and cell–cell recognition	Polysaccharides, proteins and DNA
Cohesion of biofilms	Forms a hydrated polymer network (the biofilm matrix), mediating the mechanical stability of biofilms (often in conjunction with multivalent cations) and, through the EPS structure (capsule, slime or sheath), determining biofilm architecture, as well as allowing cell–cell communication	Neutral and charged polysaccharides, proteins (such as amyloids and lectins), and DNA
Retention of water	Maintains a highly hydrated microenvironment around biofilm organisms, leading to their tolerance of dessication in water-deficient environments	Hydrophilic polysaccharides and, possibly, proteins
Protective barrier	Confers resistance to nonspecific and specific host defences during infection, and confers tolerance to various antimicrobial agents (for example, disinfectants and antibiotics), as well as protecting cyanobacterial nitrogenase from the harmful effects of oxygen and protecting against some grazing protoza	Polysaccharides and proteins
Sorption of organic compounds	Allows the accumulation of nutrients from the environment and the sorption of xenobiotics (thus contributing to environmental detoxification)	Charged or hydrophobic polysaccharides and proteins
Sorption of inorganic ions	Promotes polysaccharide gel formation, ion exchange, mineral formation and the accumulation of toxic metal ions (thus contributing to environmental detoxification)	Charged polysaccharides and proteins, including inorganic substituents such as phosphate and sulphate
Enzymatic activity	Enables the digestion of exogenous macromolecules for nutrient acquisition and the degradation of structural EPS, allowing the release of cells from biofilms	Proteins
Nutrient source	Provides a source of carbon-, nitrogen- and phosphorus-containing compounds for utilization by the biofilm community	Potentially all EPS components
Exchange of genetic information	Facilitates horizontal gene transfer between biofilm cells	DNA
Electron donor or acceptor	Permits redox activity in the biofilm matrix	Proteins (for example, those forming pili and nanowires) and, possibly, humic substances
Export of cell components	Releases cellular material as a result of metabolic turnover	Membrane vesicles containing nucleic acids, enzymes, lipopolysaccharides and phospholipids
Sink for excess energy	Stores excess carbon under unbalanced carbon to nitrogen ratios	Polysaccharides
Binding of enzymes	Results in the accumulation, retention and stabilization of enzymes through their interaction with polysaccharides	Polysaccharides and enzymes

Figure 5. Components of EPS and their roles. Taken from [6],
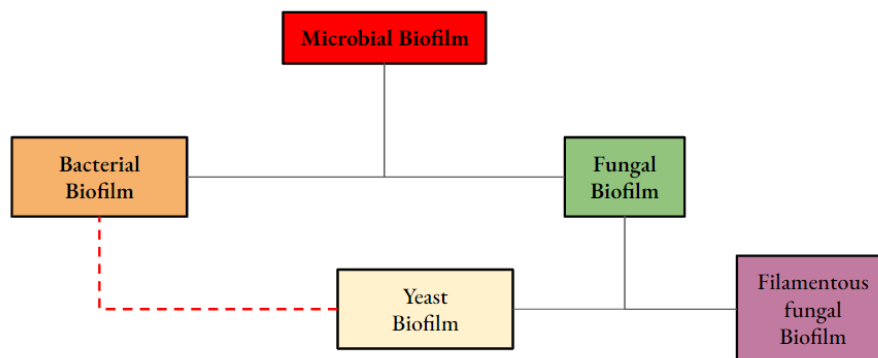
1.4 Classification of biofilms

Figure 6. Biofilm classification

Majority of the biofilms can be classified into fungal and bacterial biofilms. Under fungal biofilms, there are two main subgroups: yeast biofilms and filamentous fungal biofilms. The process of formation of bacterial and yeast biofilms are the same while that of filamentous fungal biofilms is very different.

1.4.1 Similarities and differences between bacterial and fungal biofilms

a) Similarities in the process of formation

The process of formation of bacterial and fungal biofilms are similar in the sense that the whole process can be divided into several stages (Fig. 7) where at first individual cells find their way to a surface and attach themselves to it. Then each cell starts to grow and start to produce EPS. During this growth and EPS production, the cells begin to cluster together. This cluster starts to mature and grows in thickness until external factors lead to detachment of some cells, starting the cycle again.

b) Differences in the process of formation

To form a bacterial or yeast biofilm, the microbes undergo reproduction and each cell separates into two daughter cells (binary fission). This process happens for all the cells leading to increased EPS production and collective motion. On the other hand, to form a filamentous fungal biofilm, the fungal spore does not undergo binary fission. Rather, it starts to extend into a filament-like structure (hypha) and create new branches. These branches fuse with other branches forming an interconnected network of filaments. Further details of filamentous fungal biofilm formation is discussed in the next section.

Another differentiating point is that fungi has more than one planktonic form: spores, sporangia, hyphal fragments. There is also an aerial component in fungal biofilms which is not found in bacterial biofilms. For example, the hyphal filaments can extend into the air or the fungal spores can float in the air before attaching to a surface [8].
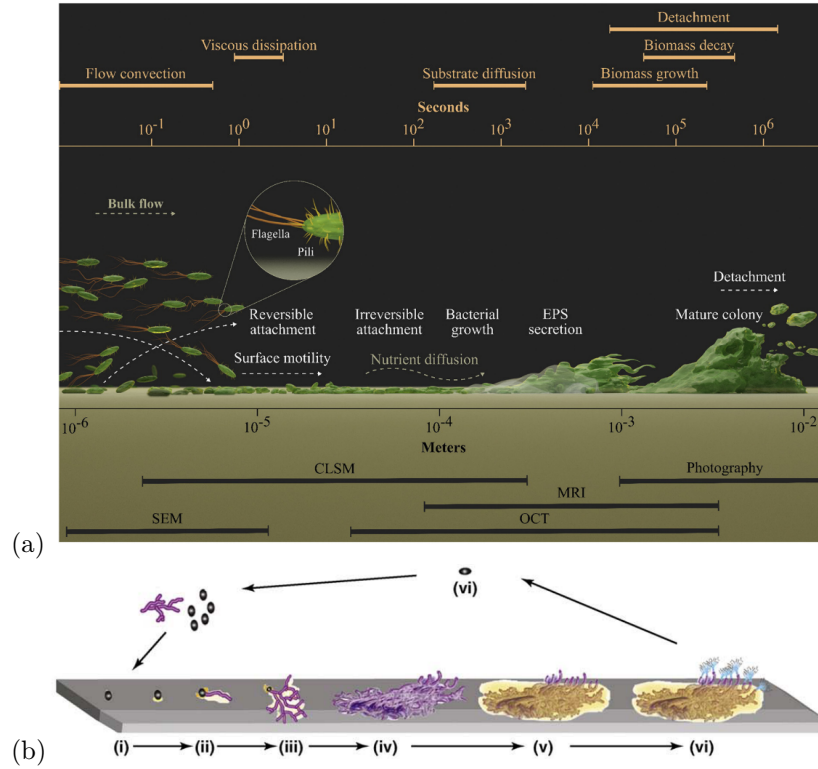

Figure 7. (a) Bacterial biofilm life-cycle along with the relevant scales. Image taken from ref: Hydrodynamics and surface properties influence biofilm proliferation. (b) Filamentous fungal biofilm life-cycle. (i) adsorption (ii) active attachment (iii) microcolony (iv) mycelial development (v) mature biofilm, and (vi) dispersal of planktonic forms. Image taken from [8]

2 Filamentous Fungal Biofilms

2.1 Stages of formation

In the previous section, the formation of filamentous fungal biofilm was introduced. This section will discuss the details (Fig. 8). When a fungal spore is dispersed, it remains dormant at first. When there are enough nutrients, the spore comes out of dormancy and swells up. During the swelling, a polarity is established which acts as a guiding hand for the extension. This leads to the growth of the filaments which happens due to the extension of the tips resulting from the uptake of cellular material. There are subcellular organelles and molecular motors inside the tip which gets activated when nutrients are sensed in the vicinity. This leads to protein synthesis and creation of new cell walls. As growth happens, the hyphae divides into branches. The hyphae can branch at the tip or at the intermediate regions (Fig. 9) or can fuse into other hyphae or tips (Fig. 10). This fusion is called *Anastomosis*.
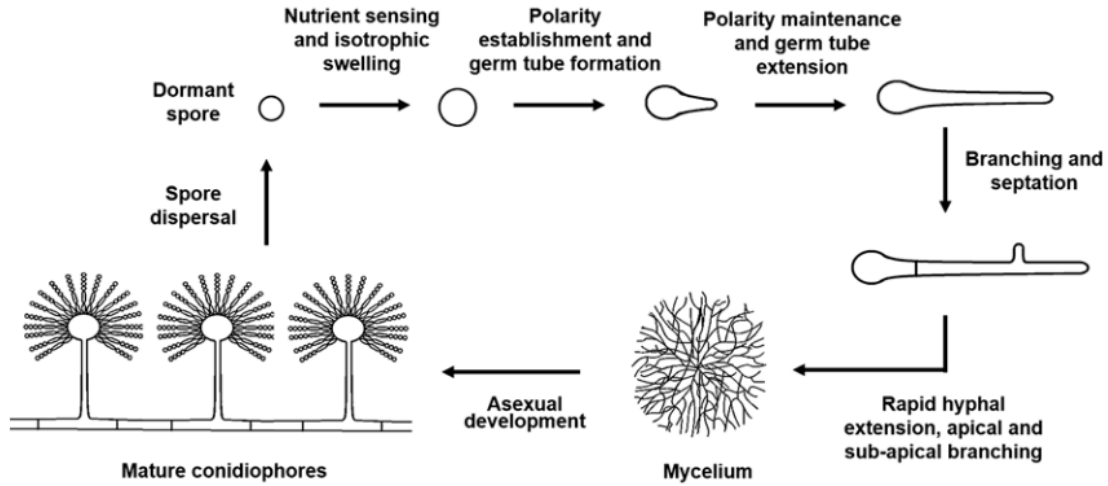

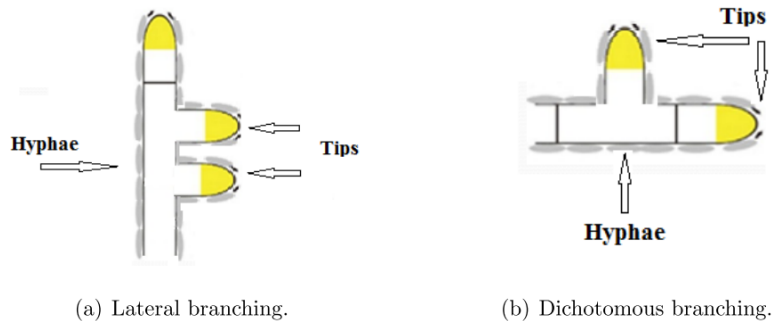**Figure 8.** Typical development of filamentous fungal biofilm. Image taken from [9]

(a) Lateral branching.

(b) Dichotomous branching.

Figure 9. Types of branching. Image taken from [10]

(a) Tip-Hyphae anastomosis.
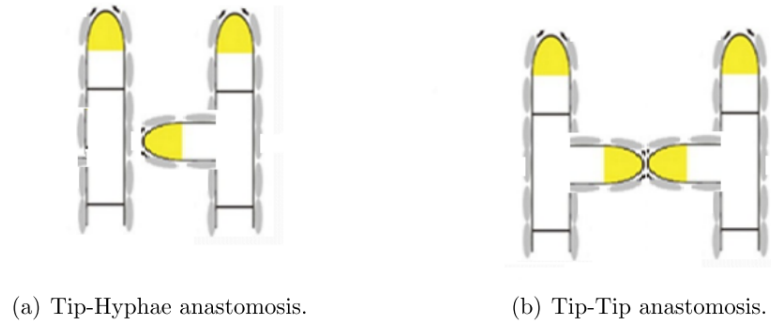
(b) Tip-Tip anastomosis.

Figure 10. Types of fusion. Image taken from [10]

Usually there are three different types of hyphae formed: aerial, biofilm and penetrative (Fig. 11). This thesis will focus on biofilm hyphae. The hyphae at the interface of biofilm and substrate (over which the spores are dispersed) has access to nutrients. This leads to a steep concentration gradient within the substrate. If the rate of intake is high, then the biofilm will start to grow thicker with the regions far away from the substrate lacking access to nutrients. At the air-biofilm interface, the hyphae take up oxygen to grow. Since the process of intake of oxygen is diffusion, it is a slow process. This leads to the hyphae at biofilm-substrate interface starving for oxygen. This gradient in concentration across the biofilm can determine how the biofilms grows. The aerial hyphae can be squashed down by agitating the system after some static growth (Fig. 12).
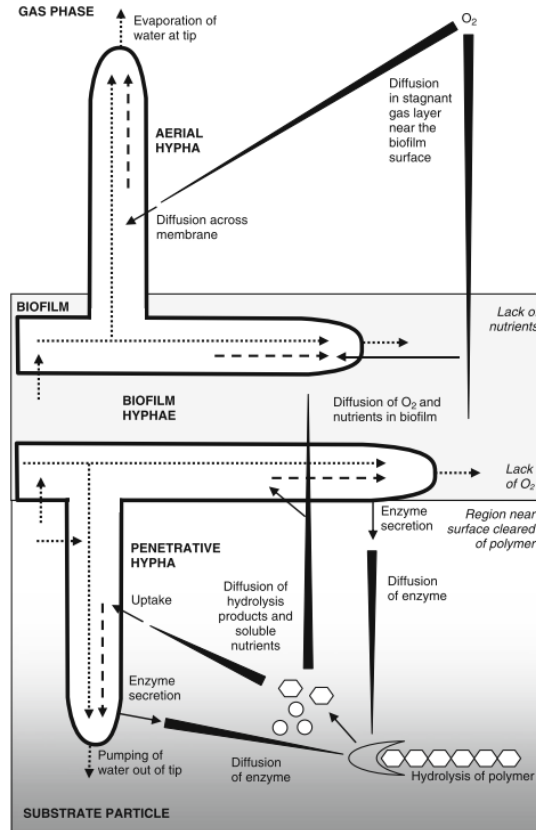

Figure 11. Phenomena involved in the growth of biofilm, penetrative, and aerial hyphae. "Long triangles" represent diffusion down concentration gradients. "Dotted arrows" represent flow of water or cytoplasm. "Dashed arrows" represent transport of vesicles. Image and caption taken from [11]
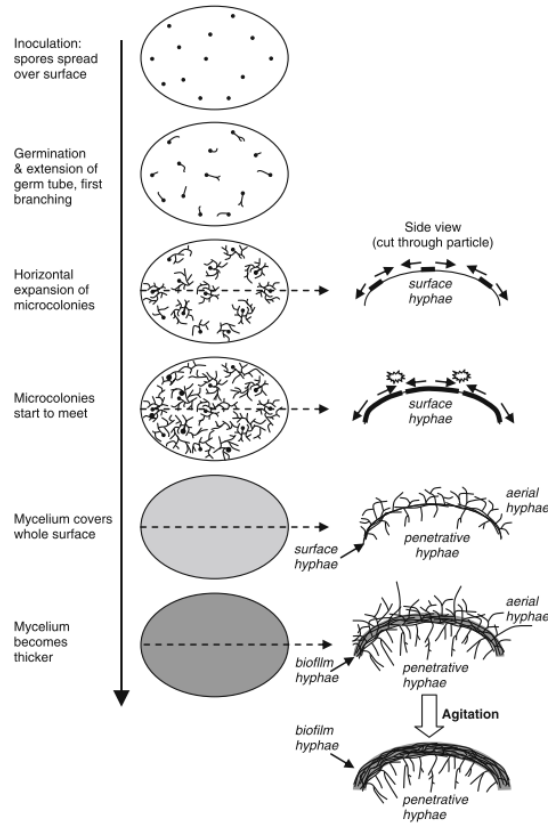
10

Figure 12. Growth of filamentous fungal biofilm on a surface leading to formation of different types of hyphae: aerial hyphae, biofilm hyphae and penetrative hyphae. Taken from [11]

2.2 Classification of Mathematical models

Mathematical models of filamentous fungal biofilms are classified into three types based on the scale: [11]

- Microscale models (μm)

  This is suited for cases when a part of an individual hyphae and processes inside it needs to me modelled. Best suited for modelling intracellular transport which are related to tip growth. The molecular motors near the hyphal tips responsible for the extension and intake can be investigated.

- Mesoscale models (mm to cm)

  This is for modelling anything between a single hyphae and a biomass. Best suited to model growth of colonies along with the effect of extracellular nutrients on the growth. Branching and direction-changing growth can be covered.

- Macroscale models (cm to m)

  To model a biomass or larger systems. This is suitable to study the performance of the bioreactor on which the biofilm is being grown. Mass and heat transfer between particles can be studied.

In this thesis, a mesoscale model is considered.

2.3 Boswell's model

This thesis will discuss a modified model based on [12][13]. In this model the mycelium/fungal biomass is considered to be made of distribution of three main components: Active hyphae, Inactive hyphae and Hyphal tips [10].

- *Active Hyphal density (ρ)*

  This represents the hyphae/filaments which are actively involved in taking in nutrients from the surroundings to grow. This intake of nutrients from the external environment and movement of nutrients inside the hyphae is called *Translocation*. Active hyphae are the growing part of the biofilm.

- *Inactive Hyphal density (ρ')*

  The hyphae which remain dormant or are not involved in branching or translocation are Inactive hyphae. This is common when a hyphae fuses into another hyphae which means it does not have scope to grow more. This model does not consider the reactivation of inactive hyphae which has been observed experimentally when there is temporal heterogeneity in nutrients [14]. So we assume that anastomosis leads to inactive hyphae.

- *Hyphal tip density (n)*

  These are the ends of each hyphae which lead the growth process.

The biomass grows by taking in nutrients from the surroundings. The nutrients inside the hyphae is represented by s_i − internal substrate concentration, and the nutrients in the surrounding is represented by s_e − external substrate concentration. This model does not consider the effects of the physical boundaries on fungal growth. The external environment is considered to be two-dimensional as a result of the assumption that the gradients along the depths are negligible. Therefore, the whole mycelium can be approximated as a two-dimensional entity. It has been observed experimentally that the mycelium has a fractal structure [15]. This means that the nutrient diffusion time inside the mycelium is less than in the exterior. This can be modelled by taking the diffusion coefficient inside mycelium to be greater than that in the exterior.

2.3.1 Formulation

The main features of this model and the corresponding PDEs are: (written in terms of J and f which denote the flux (migration) terms and reaction (creation/loss) terms respectively)[12][13]

i. New hyphae are created by movement of tips

> change in active hyphae = new hyphae(convection and diffusion of tips) − inactivation of active hyphae
>
> $$\frac{\partial \rho}{\partial t} = f_\rho(\rho, \rho', n, s_i, s_e)$$

Since the tip is the motile part of the mycelium, hyphae can be considered to be the trail

left at the wake of the tip motion. So number of tips multiplied by the distance moved by the tip in a short period of time (velocity) gives the amount of hyphae created. Therefore, the total hyphal length per unit time can be represented by the absolute value of the *tip flux*: $|J_n|$. Some parts of the mycelium become inactive and as per our assumption stated earlier, anastomosis leads to inactivation. Inactivation is modelled by a reaction term with rate d_ρ. Incorporating all these as the f_ρ term gives

$$\frac{\partial \rho}{\partial t} = |J_n(\rho, \rho', n, s_i, s_e)| - d_\rho \rho$$

Experimental observations show that the hyphae grow in a straight line for the most part. They (tips) also show small random changes in direction. These two processes are modelled by a convective and a diffusive term respectively inside J_ρ. It is important to note that the growth happens only when the hyphae gets the energy (internal substrate). So if $s_i = 0$, then $J_\rho = 0$. The convective flux happens in such a way that the hyphae avoids its own trail, or in other words, growth proceeds in the direction of decreasing hyphal density. So the convective term is: $-nv(s_i, \nabla \rho)$ where v is the velocity vector assumed to be a bilinear function of s_i and $\nabla \rho$. The diffusive term is modelled as: $-D_n(s_i) \nabla n$ where $D_n(s_i)$ is the diffusion coefficient assumed to be a linear function of s_i. Combining these two gives $J_n = -nvs_i \nabla \rho - D_n s_i \nabla n$

$$\Rightarrow \quad \frac{\partial \rho}{\partial t} = |nvs_i \nabla \rho + D_n s_i \nabla n| - d_\rho \rho \tag{1}$$

ii. Hyphae can become inactive and either remain inactive or die

> change in inactive hyphae = inactivation of active hyphae − death of inactive hyphae
>
> $$\frac{\partial \rho'}{\partial t} = f_{\rho'}(\rho, \rho', n, s_i, s_e)$$

The rate at which active hyphae become inactive is d_ρ and the rate at which the inactive hyphae die is d_i. In the absence of detailed experimental evidence and to be consistent with the reaction term in Eq. (1), both processes are modelled as: $f_{\rho'} = d_\rho \rho - d_i \rho'$. This gives,

$$\Rightarrow \quad \frac{\partial \rho'}{\partial t} = d_\rho \rho - d_i \rho' \tag{2}$$

iii. Hyphae and tips can either branch out or fuse via anastomosis

> change in hyphal tips = tip influx and outflux + branching of active hyphae − anastomosis
>
> $$\frac{\partial n}{\partial t} = -\nabla . J_n(\rho, \rho', n, s_i, s_e) + f_\rho(\rho, \rho', n, s_i, s_e)$$

The term f_ρ corresponds to the creation and loss of hyphae. Creation of hyphae is the branching process, and as seen in Fig. 9, there are two types. The exact process that leads to branching is still an area of research but a highly probable mechanism is the turgor pressure from the accumulation of ionic gradients and internal substrate at the tips. Assuming this, the branching requires internal substrate and a linear relationship between branching rate and s_i is taken for simplicity; αs_i is the per-unit length branching rate. This gives us $\alpha s_i \rho$

13

to be the creation term. Loss of hyphae is the anastomosis process (Fig. 10). Anastomosis depends on the tip density (n). So the rate of fusion is taken to be linearly dependent on n. This gives us $-\beta n\rho$ as the loss term. With tip flux (J_n) from Eq. (1),

$$\Rightarrow \quad \frac{\partial n}{\partial t} = \nabla.(v s_i n \nabla \rho + D_n s_i \nabla n) + \alpha s_i \rho - \beta n \rho \tag{3}$$

iv. Tip extension and growth are influenced by the internal nutrients

---

change in internal substrate = active and passive translocation + nutrient intake by hyphae from exterior − hyphae maintanence costs − hyphae growth cost − active translocation cost

$$\frac{\partial s_i}{\partial t} = -\nabla.\,[J_i^{\mathrm{passive}}(\rho, \rho', n, s_i, s_e) + J_i^{\mathrm{active}}(\rho, \rho', n, s_i, s_e)] + f_i(\rho, \rho', n, s_i, s_e)$$

Here, f_i is the absorption and loss of internal substrate. The process of intake of substrate is an autocatalytic process: internal substrate is used to absorb further substrate via active transport. So, the intake of nutrient depends on the amount of hyphae, amount of internal substrate, and the amount of external substrate available. Again, for simplicity, linear dependence is considered, giving us: $c_1 s_i \rho s_e$. The biomass uses energy (here, substrate) for: intake, maintanence and growth. Using energy has costs associated with it. Intake cost is taken care by choosing an appropate value for c_1. Active translocation needs energy, while passive translocation does not. Active translocation cost is assumed to be proportional to the absolute value of flux of internal substrate moved : $c_4|J_i^{\mathrm{active}}|$. Biomass growth happens due to the energy to extend the tips and therefore the cost is proportional to the tip flux: $c_2|J_n|$. Maintanence cost is included in the growth cost. We get $f_i = c_1 s_i \rho s_e - c_2|J_n(\rho, \rho', n, s_i, s_e)| - c_4|J_i^{\mathrm{active}}(\rho, \rho', n, s_i, s_e)|$. See Table 1 for definitions of the parameters.

Passive translocation is the major process behind the redistribution of internal substrate. The passive flux of internal substrate through the biomass will be dependent on the hyphal density; dense mycelium sees higher flow. So, passive flux is linearly proportional to ρ: $J_i^{\mathrm{passive}} = -D_i \rho \nabla s_i$. Active translocation is the process behind tip extension. Tip extension requires enough energy (internal substrate). It is logical to assume that the active flux will be dependent on the tip density; greater the number of tips, greater the internal substrate demand. To show that the substrate is moving through the biomass, we assume a linear dependence on ρ. So active flux is given as: $J_i^{\mathrm{active}} = D_a \rho s_i \nabla n$. Combining all these, we get:

$$\Rightarrow \quad \frac{\partial s_i}{\partial t} = \nabla.(D_i \rho \nabla s_i - D_a \rho s_i \nabla n) + c_1 s_i \rho s_e - c_2|v s_i n \nabla \rho + D_n s_i \nabla n| - c_4|D_a \rho s_i \nabla n| \tag{4}$$

v. Internal nutrients are different than external nutrients

---

change in external substrate = external substrate diffusion − nutrient intake by hyphae from exterior

$$\frac{\partial s_e}{\partial t} = -\nabla.J_e(\rho, \rho', n, s_i, s_e) + f_e(\rho, \rho', n, s_i, s_e)$$

The term f_e describes the substrate depletion and therefore must be similar in form as the substrate absorption (f_i): $f_e = -c_3 s_i \rho s_e$. Keeping in mind the intake cost discussed above, the value of $c_1 < c_3$: external substrate is not completely converted into internal substrate.

The movement of external substrate (s_e) is modelled as a standard diffusion: $J_e = -D_e \nabla s_e$. This gives,

$$\Rightarrow \quad \frac{\partial s_e}{\partial t} = D_e \nabla^2 s_e - c_3 s_i \rho s_e \tag{5}$$

Eqs. $(1)-(5)$ are a set of five coupled equations of mixed parabolic-hyperbolic type. The definition of the parameters in the equation are given in Table 1.

Parameters	Description
v	Directed tip velocity
d_ρ	Hyphal inactivation rate
d_i	Inactive Hyphae loss rate
α	Branching rate
β	Anastomosis rate
c_1	Uptake rate of external substrate
c_2	Growth rate - amount of substrate required to extend a hyphal tip
c_3	Uptake of external substrate
c_4	Active translocation cost
D_n	Tip avoidance cost
D_i	Internal substrate diffusion coefficient
D_a	Active translocation rate
D_e	External substrate diffusion coefficient

Table 1. Parameters

3 Simulation & Results

3.1 Geometry

The simulations are performed in COMSOL Multiphysics software. A circular domain of radius 2cm with a smaller circle of radius 0.2cm is built (See Fig. 13). The smaller circle is the inoculation site. Physics-controlled meshing is used with the Finer element size option (Fig. 13).
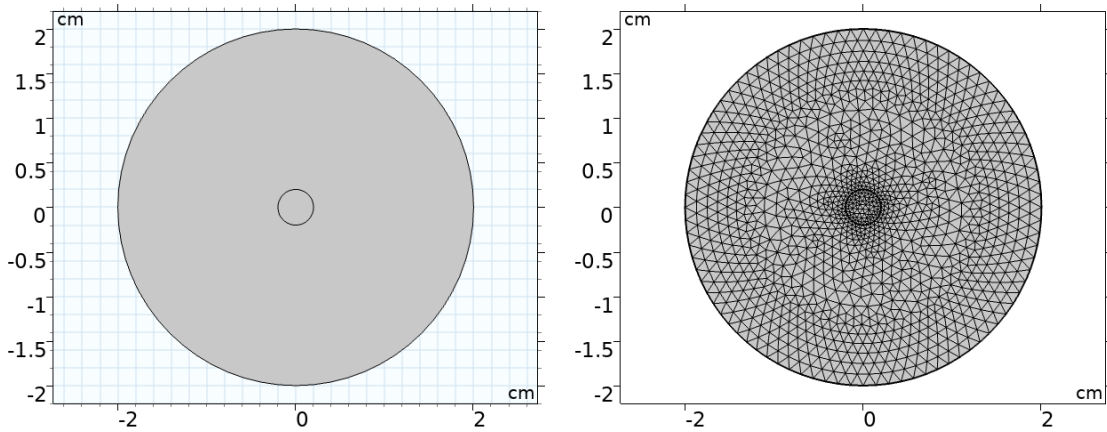

Figure 13. Geometry and meshing used for simulations.

15

3.2 Model set-up (Initial and Boundary conditions)

Each of the Eqs. (1)-(5) are set up using the Coefficient Form PDE Phyiscs module. Coefficient Form PDE is of the form:

$$e_a \frac{\partial^2 u}{\partial t^2} + d_a \frac{\partial u}{\partial t} + \nabla.(-c\nabla u - \alpha u + \gamma) + \beta.\nabla u + a u = f$$

where $u = [\rho, \rho', n, s_i, s_e]^T$ and $\nabla = \left[\frac{\partial}{\partial x}, \frac{\partial}{\partial y}\right]$. So, the model equations can be entered by defining $e_a = a = \beta = \gamma = 0$, along with

$$d_a = \begin{pmatrix} 1 & 0 & 0 & 0 & 0 \\ 0 & 1 & 0 & 0 & 0 \\ 0 & 0 & 1 & 0 & 0 \\ 0 & 0 & 0 & 1 & 0 \\ 0 & 0 & 0 & 0 & 1 \end{pmatrix},$$

$$c = \begin{pmatrix} 0 & 0 & 0 & 0 & 0 \\ 0 & 0 & 0 & 0 & 0 \\ 0 & 0 & D_n s_i & 0 & 0 \\ 0 & 0 & 0 & D_i \rho & 0 \\ 0 & 0 & 0 & 0 & D_e \end{pmatrix},$$

$$\alpha = \begin{pmatrix} 0 & 0 & 0 & 0 & 0 \\ 0 & 0 & 0 & 0 & 0 \\ 0 & 0 & v s_i \nabla \rho & 0 & 0 \\ 0 & 0 & 0 & -D_a \rho \nabla n & 0 \\ 0 & 0 & 0 & 0 & 0 \end{pmatrix},$$

$$f = \begin{pmatrix} |n v s_i \nabla \rho + D_n s_i \nabla n| - d_\rho \rho \quad [\mathrm{cm}^{-1}\mathrm{day}^{-1}] \\ d_\rho \rho - d_i \rho' \quad [\mathrm{cm}^{-1}\mathrm{day}^{-1}] \\ \alpha s_i \rho - \beta n \rho \quad [\mathrm{cm}^{-2}\mathrm{day}^{-1}] \\ c_1 s_i \rho s_e - c_2 |v s_i n \nabla \rho + D_n s_i \nabla n| - c_4 |D_a \rho s_i \nabla n| \quad [\mathrm{mol\,cm}^{-2}\mathrm{day}^{-1}] \\ -c_3 s_i \rho s_e \quad [\mathrm{mol\,cm}^{-2}\mathrm{day}^{-1}] \end{pmatrix}$$

No Flux boundary condition is applied to the boundaries of the outer circle. For each of the five quantities, initial conditions are as follows:

$$\rho_{\mathrm{initial}} = \rho_0 \, f(r),$$

$$\rho'_{\mathrm{initial}} = \rho'_0,$$

$$n_{\mathrm{initial}} = n_0 \, f(r),$$

$$s_{i_{\mathrm{initial}}} = s_{i_0} \, f(r),$$

$$s_{e_{\mathrm{initial}}} = s_{e_0},$$

where $f(x) = 1 - \tanh(800000 r^2)$. The initial conditions represent the inoculum to be distributed in such a way that the density/concentration value is maximum at the centre of the inoculation site and falls to zero smoothly at $r = 0.2$cm according to $f(r)$ (see Fig. 14). The values of the parameters and the initial conditions in the model equations are given in Table 2.

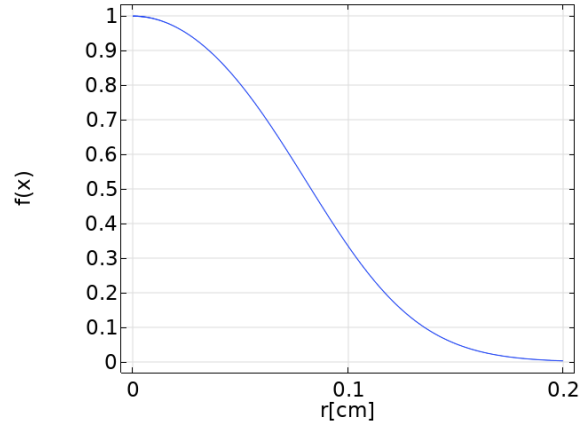**Figure 14.** Smoothening function

Parameters	Description	Value
v	Directed tip velocity	0.5
d_ρ	Hyphal inactivation rate	0.5
d_i	Inactive Hyphae loss rate	0
α	Branching rate	10^3
β	Anastomosis rate	10^4
c_1	Uptake rate of external substrate	900
c_2	Growth rate - amount of substrate required to extend a hyphal tip	1
c_3	Uptake of external substrate	10^3
c_4	Active translocation cost	10^{-8}
D_n	Tip avoidance cost	0.1
D_i	Internal substrate diffusion coefficient	10
D_a	Active translocation rate	10
D_e	External substrate diffusion coefficient	0.3456
ρ_0	initial active hyphal density	0.1 [1/cm]
ρ_0'	initial inactive hyphal density	0 [1/cm]
n_0	initial hyphal tip density	0.1 [1/cm^2]
s_{i_0}	initial internal substrate concentration	0.4 [mol/cm^2]
s_{e_0}	initial external substrate concentration	0.3 [mol/cm^2]

Table 2. Parameter values and initial conditions.

3.3 Results

The five model equations are solved simultaneously using time-dependent solver on the two-dimensional domain. The solver uses Backward Differentiation Formula (BDF) method with *free* time-stepping which allows the solver to take time steps as needed for the specific tolerance. The analysis of the solution is done via various plots as discussed below.

3.3.1 Surface Plots

Surface plots show how the quantities evolve with time over the two-dimensional domain. Fig. 15 shows the growth of the biofilms over the period of 10 days. More specifically, it shows how each component of the biofilm grows. The solutions can be seen as travelling waves moving radially outward from the inoculation site which is at the centre of the domain. In Fig. 15(a), the Active Hyphal Density decreases as it spreads out occupying the domain. In contrast, the Inactive Hyphal Density (Fig. 15(b)) increases as the biofilm grows. This is in accordance with the logic that the active hyphae starts to become inactive at a specific rate starting from the centre. Since hyphal

tips lead the growth, Fig. 15(c) shows the spreading of the tips. Initially, the tips are highly concentrated at the centre and as the biofilm grows, new tips emerge at the boundary of the growing front. The Internal Substrate concentration (Fig. 15(d)) looks similar to the Hyphal tip density solution, and this could be due to the way in which the model is formulated. Finally, the External Substrate concentration (Fig. 15(e)) is the complement of the Internal Substrate concentration plot because as the hyphae grows, it takes in nutrients from the external substrate and subsequently increasing the internal substrate. But the surface plot does not give us any more information on the dynamics of the growth of each of the quantities. So, we move to other plots.
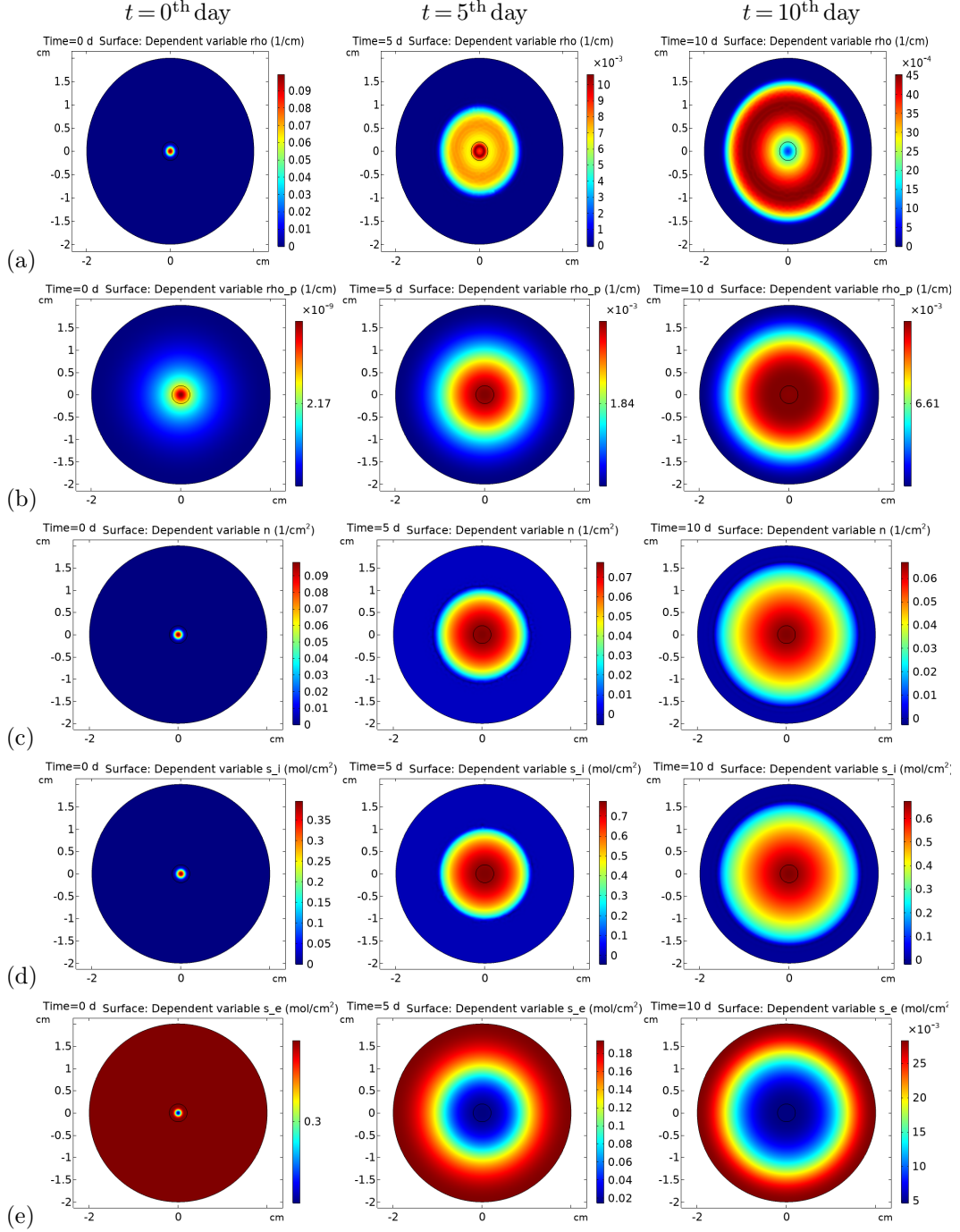

Figure 15. Surface plots of (a) Active Hyphal Density, (b) Inactive hyphal density, (c) Hyphal tip density, (d) Internal substrate concentration, and (e) External substrate concentration at different time instants as shown.

18

3.3.2 Point plots

To know how each of the quantities are affected by changes in the initial condition of external substrate concentration ($s_{e_{\text{initial}}}$), all of them are plotted at a point $(x, y) = (0.4\text{cm}, 0\text{cm})$ (see Fig. 16(a),(b)) against time. $s_{e_{\text{initial}}}$ is given values of $0.29, 0.30, 0.40, 0.60$. Point to note is that the external substrate is kept homogeneous as a start to get the sense of the growth. In Fig. 16(b), the peak in Active Hyphal density reaches quicker for $s_e = 0.6$ when compared to others. Consequently, the Inactive Hyphal density also reaches a higher value for $s_e = 0.6$. The Hyphal Tip density and Internal Substrate concentration values follow a very similar trend where there is an initial rise in magnitude followed by a steady decrease. The External Substrate concentration falls rapidly for $s_e = 0.6$ case. This means that the biofilm grows faster in the presence of a higher external substrate concentration. Overall, the growth seems to start after a day which matches most experimental observations.
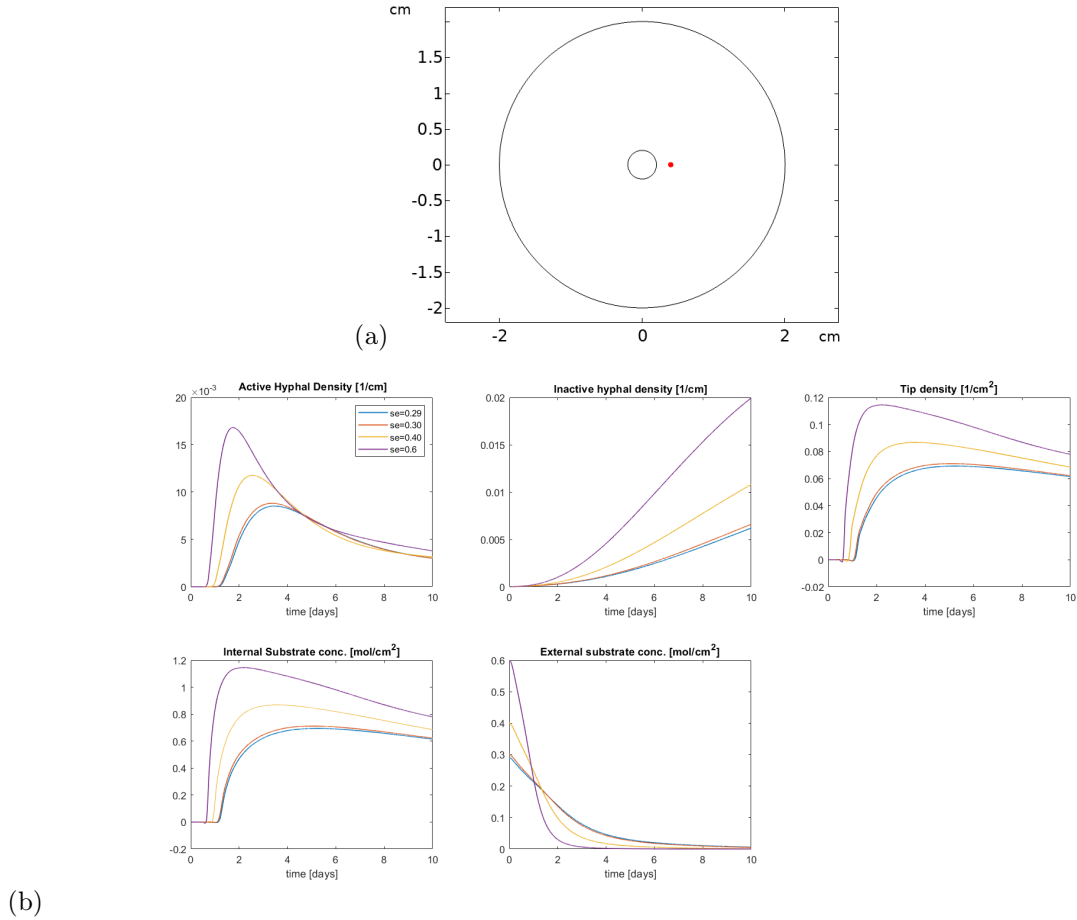

(a)

(b)

Figure 16. Point plot of the quantities for different initial External Substrate concentration (s_e) values. (a) The red dot at $(x, y) = (0.4\text{cm}, 0)$ depicts the point at which the quantities are plotted against time. (b) Point plots.

Fig. 17 shows how few quantities fare against other quantities at the same point shown in Fig. 16(a). Active Hyphal density spikes initially when the inactive hyphal density is negligibly small. As growth happens, hyphae starts to become inactive and that leads to a steady decrease in Active hyphal density (Fig. 17(a)). A higher initial External substrate concentration leads to a higher initial spike in Active hyphal density and then a longer steady decrease in active hyphal density. When External substrate and Active Hyphal density are plotted against each other (Fig. 17(b)), there appears to be a threshold value of s_e crossing which there is spike in the Active Hyphal density. For $s_e = 0.6$ case, the threshold is around 0.37 and as the initial s_e value is decreases, the threshold value also comes down correspondingly. The Active Hyphal density reaches a maximum when the External substrate concentration reaches a low enough value. After that there is a

decrease in active hyphal density as the External substrate gets fully depleted. Similar argument can be made for the External substrate vs Internal substrate plot (Fig. 17(c)).
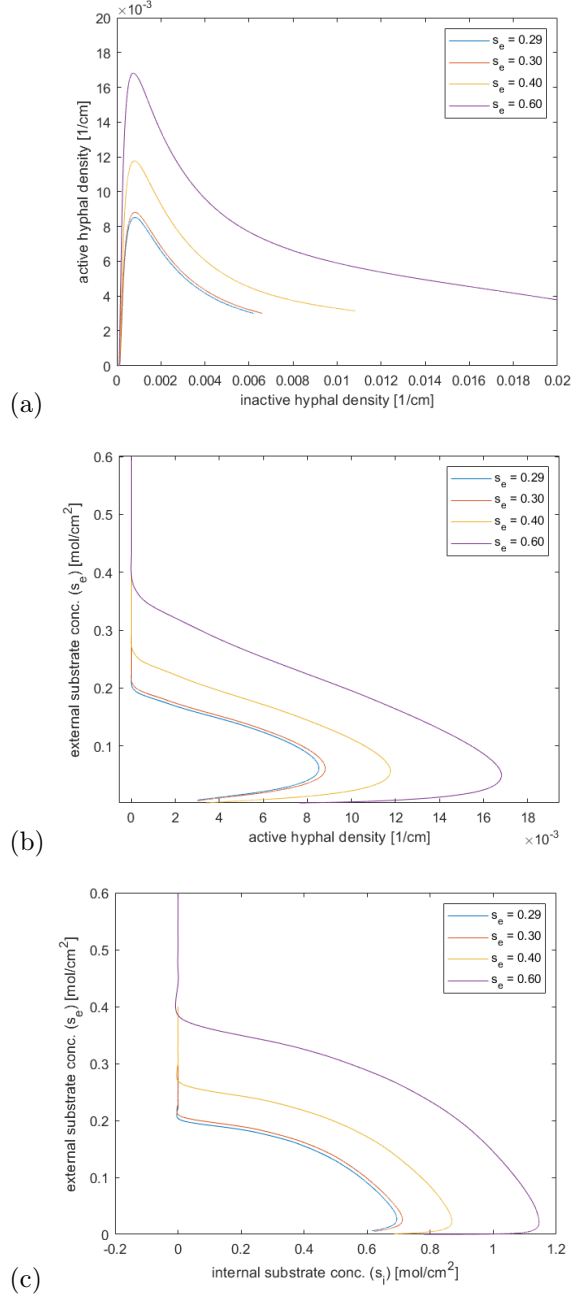

(a)

(b)

(c)

Figure 17. Point plots of a quantity against another quantity for different initial External substrate concentration (s_e) values. The point at which the quantities are plotted is the same as shown in Fig. 17(a). (a) Active hyphal density vs Inactive hyphal density, (b) s_e vs Active hyphal density, and (c) s_e vs s_i.

3.3.3 Line plots

It is a good idea to know how the profile of each of the quantities vary as growth happens. For this, the quantities are plotted along a diameter (Fig. 18(a)) at different time instants. The x-axis is the arc length starting from 0 which corresponds to $(-2\text{cm}, 0\text{cm})$ in the domain and ends at 4 which corresponds to $(2\text{cm}, 0\text{cm})$ in the domain. The Active Hyphal density starts off having a tall peak at the inoculation site (around arc length = 2cm) (Fig. 18(b)). Then as growth starts, the amplitude of the peak decreases and the base starts to spread out towards the boundaries. The

Hyphal Tip density decreases in the 1st day but increases the following days while also spreading towards the boundaries(Fig. 18(c)). The Internal Substrate concentration increases and spreads towards the boundaries (Fig. 18(d)). External substrate concentration is constant initially and its depletion starts from the centre proceeding towards the boundaries (Fig. 18(e)).
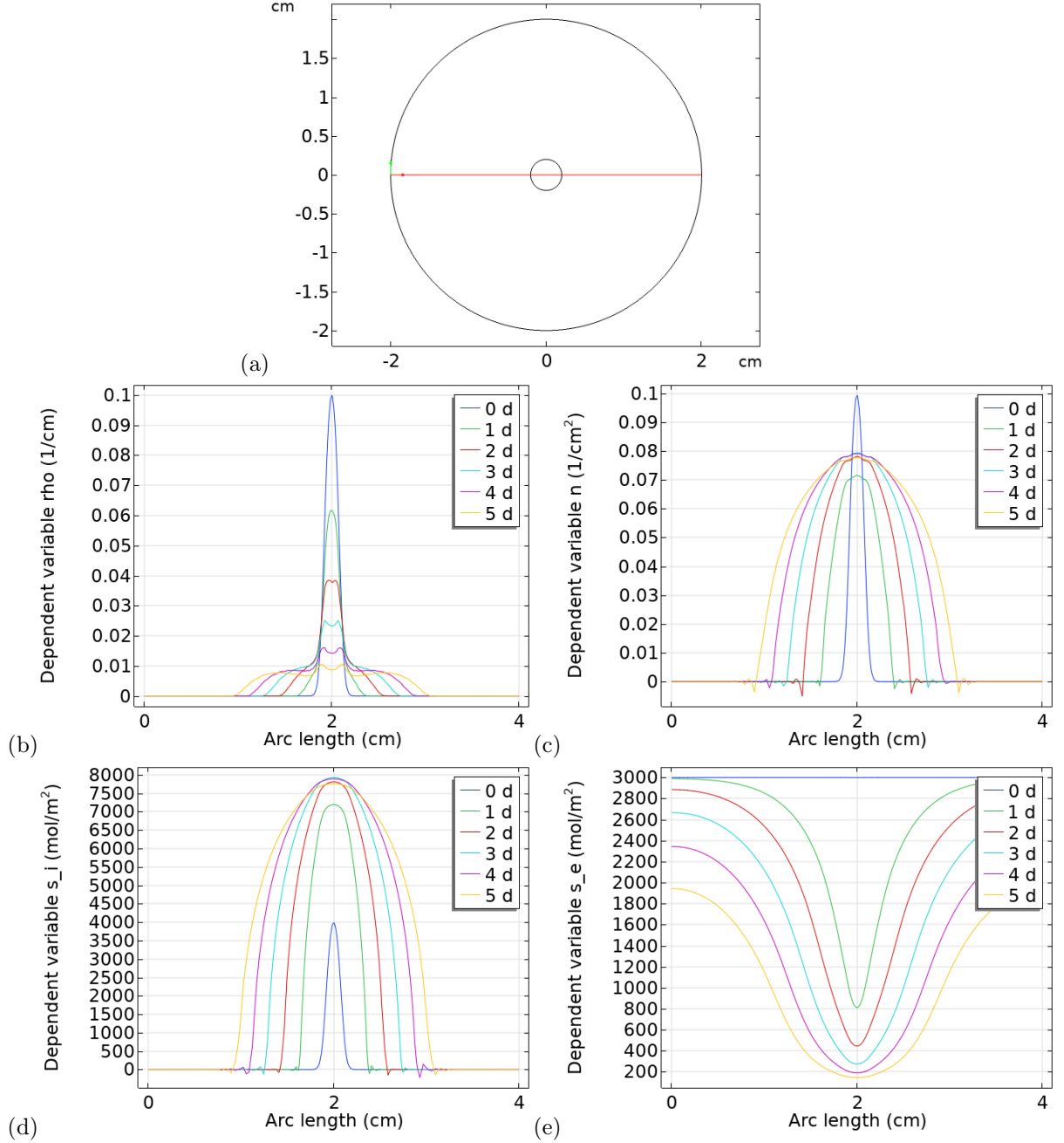

Figure 18. Line plot along the diameter of the domain for $(s_e)_0 = 0.3 \, \text{mol} / \text{cm}^2$. (a) The red line depicts the diameter along which the quantities are being plotted. Line plot of (b) Active hyphal density, (c) Hyphal tip density, (d) Internal substrate concentration, and (e) External substrate concentration at different time instants as shown in the legend.

3.3.4 Active vs Passive Translocation in Homogeneous environment

It is known that, in a heterogeneous environment, a fungi uses resources from nutrient-rich region to support its growth in nutrient-poor regions. This implies that the nutrient are being internally

transported (*translocated)* within the mycelium. There has been evidence of two different mechanisms for translocation [12][13]: Passive (diffusion-driven) and Active (metabolically-driven).

These two mechanisms are considered while formulating the model. In Eq. (4), the term $D_i \rho \nabla s_i$ correpsonds to Passive translocation and the term $D_a \rho s_i \nabla n$ corresponds to Active translocation. To differentiate between the roles of each mechanism, D_a was turned to zero for growth in a homogeneous environment ($s_{e_{\text{initial}}}$=constant). Making $D_a = 0$ means there will be no Active translocation. And, to isolate the effect of translocation, the external substrate diffusion coefficient (D_e)(see Eq. (5)) was made zero. Fig. 19 shows the results. Non-zero values of D_a and D_e are as mentioned in Table 2.

The plots in Fig. 19 show that keeping D_e non-zero and changing D_a from a non-zero value to a zero value has negligible effect on the solution (Blue and yellow lines are very close together). This means that invoking active translocation is not advantageous in a homogeneous environment. Proof that passive translocation indeed happens is in the plot with both $D_a = D_e = 0$ (red line). Since $D_e = 0$, there is no diffusion of nutrients from outside to inside. So whatever growth happens, that must be completely due to the internal substrate. Another proof that active translocation is not advantageous for growth of filamentous fungal biofilms in a homogeneous environment is shown in Fig. 20. This plots the three quantities when both $D_a = D_e = 0$ and when only $D_e = 0$. There is very negligible difference in the solutions.
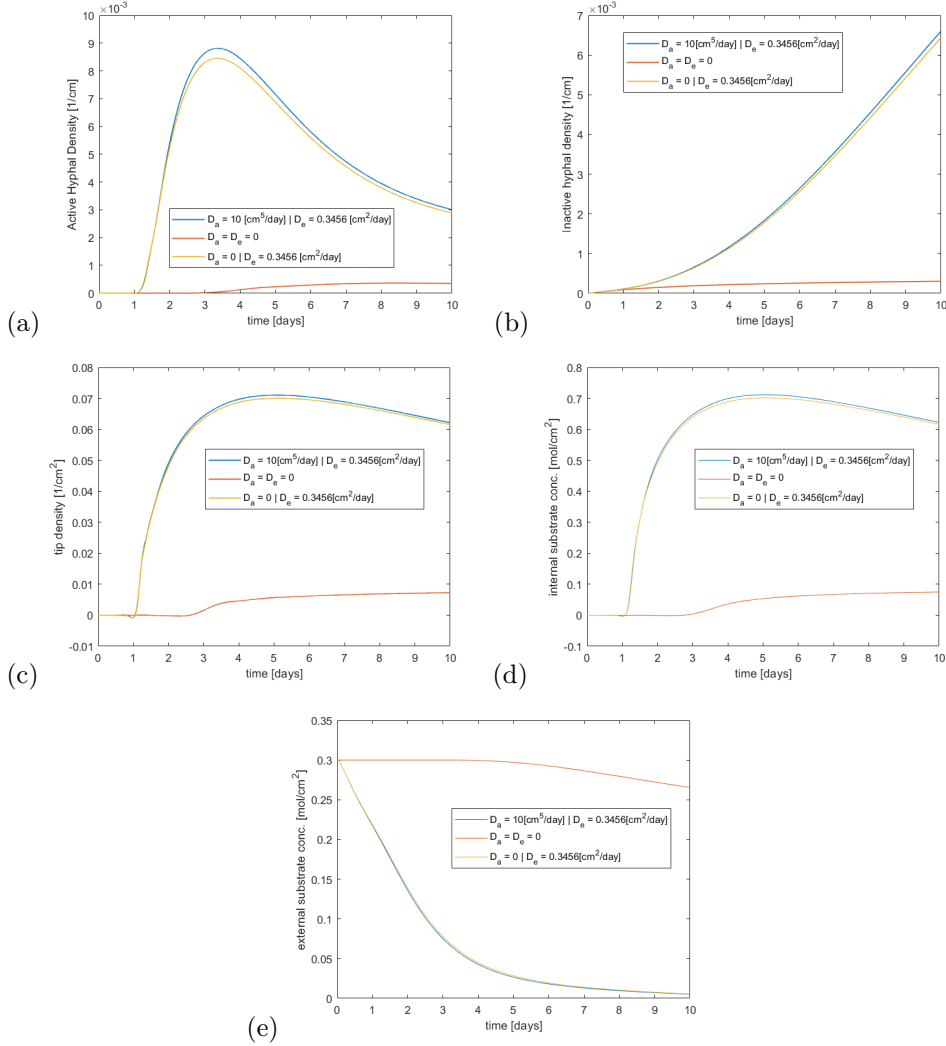

Figure 19. Point plots of (a) Active Hyphal Density, (b) Inactive Hyphal Density, (c) Hyphal Tip Density, (d) Internal Substrate Concentration, and (e) External Substrate Concentration, for different combinations of D_a and D_e values as shown in legends. $s_{e_{\text{initial}}} = 0.3 \, \text{mol/cm}^2$
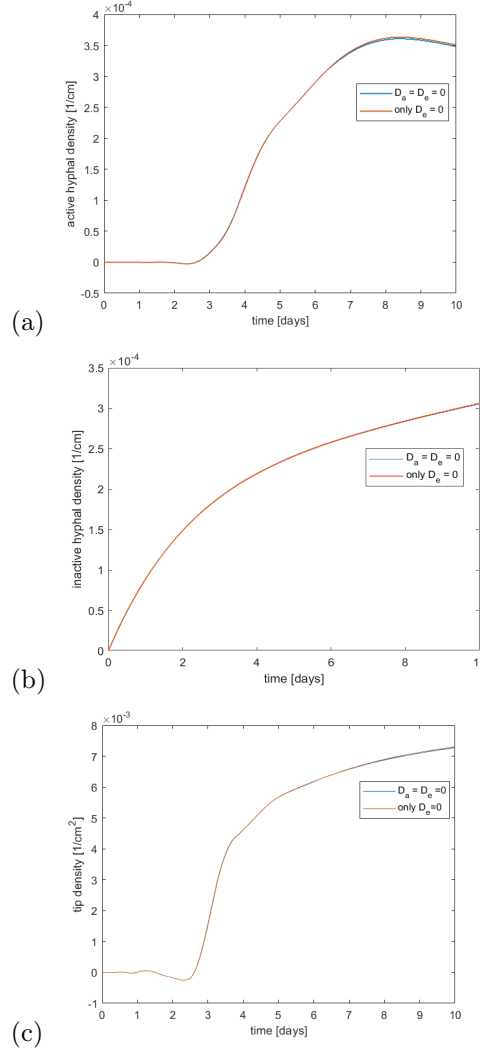
22

Figure 20. Point plots of (a) Active Hyphal density, (b) Inactive Hyphal density, and (c) Hyphal tip density, for zero and non zero values of D_a and D_e. $s_{e_{\text{initial}}} = 0.3\,\text{mol}/\text{cm}^2$

One more proof that translocation is indeed happening is given by considering a new case along with the previously mentioned ones. The new case has a Localised Resource where the External Substrate is a non-zero constant value only in the region of inoculation and is zero elsewhere (Fig. 21). In other words,

$$s_{e_{\text{initial}}} = 0.3\,\text{mol}/\text{cm}^2 \quad \text{for} \quad r \leqslant 0.2\text{cm} \text{ and zero otherwise}$$

Since there is no substrate outside of the inoculation site, the growth must be due to the already diffused nutrients from the inoculation site and internally transported. Comparing the cases of both only $D_e = 0$ (red) and only $D_e = 0$ with Localised Resource (purple), the latter shows lesser growth. This seems to tell that active translocation in a homogeneous environment uses up a lot of energythat it causes a net drain of resources. All these results are similar to that obtained in [12][13].
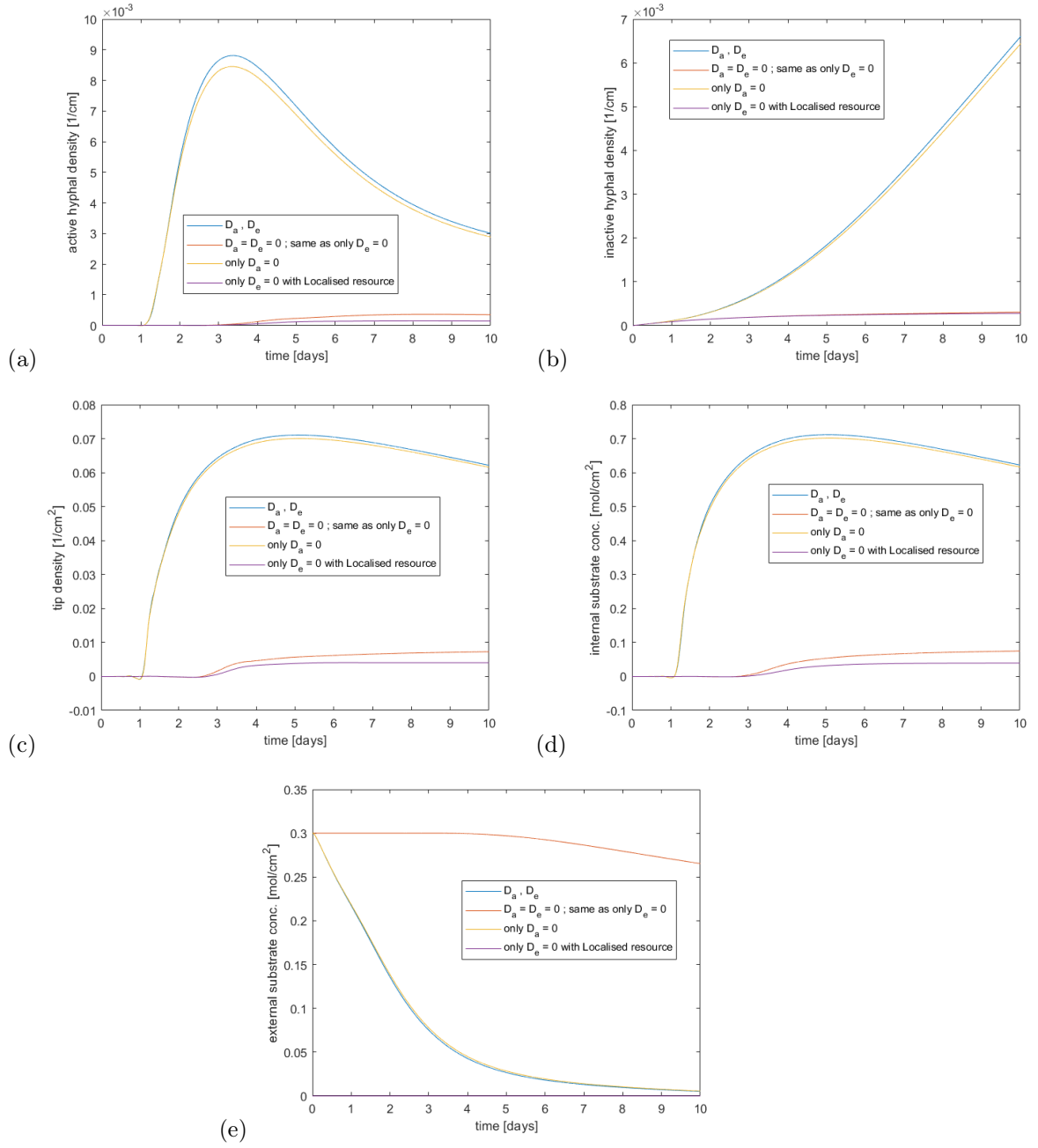
Figure 21. Point plots of (a) Active Hyphal Density, (b) Inactive Hyphal Density, (c) Hyphal Tip Density, (d) Internal Substrate Concentration, and (e) External Substrate Concentration, for different combinations of D_a and D_e values as shown in legends. $s_{e_{\text{initial}}} = 0.3\,\text{mol}/\text{cm}^2$

3.3.5 Inoculum distributed all over the domain (Homogeneous environment)

To match the experimental setup in [1] as close as possible, 16 inoculation sites each of radius 0.2cm was distributed in a symmetric manner (Fig. 22). The initial and boundary conditions are kept the same as mentioned in Section 3.2, with the only difference that instead of a single inoculation site at the centre, there are 15 more sites distributed all over the domain.

Fig. 23 shows the surface plots of all the quantities at three different time instants. The radially propagating waves from every inoculation site interact with each other. Not much information

can be gathered from the surface plots, so moving to the line plots (Fig. 24(b)) where the Total Hyphal density (= active hyphal density + inactive hyphal density), Hyphal tip density, Internal substrate concentration, and External substrate concentration are plotted along the diameter line as shown in Fig. 24(a). The common observation from these plots is that as the biofilm grows, there is a larger amount of hyphal density, tip density and internal substrate concentration near the boundaries when compared to the centre of the domain. The external substrate also matches the trend with a little higher value in the central region compared to near the boundaries (more external substrate is depleted near the boundaries). Experimental observations in [1] show that the biofilm is denser near the boundaries than at the centre.
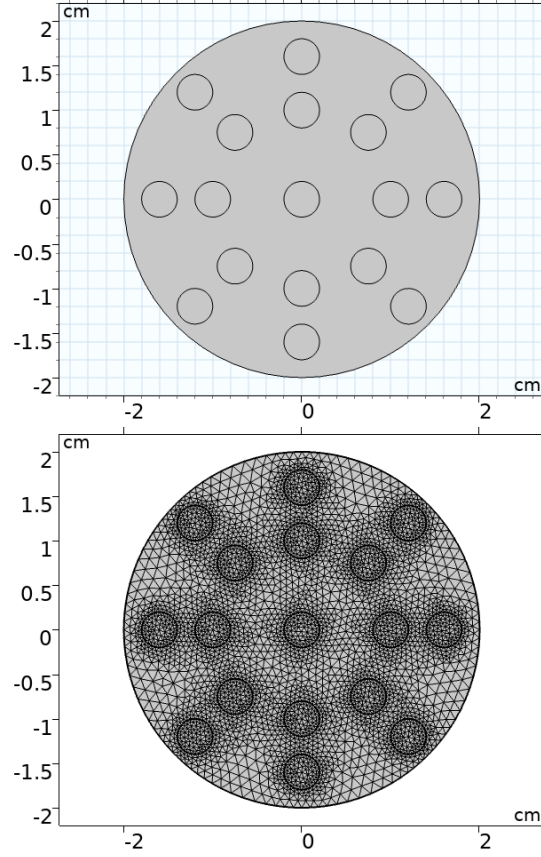

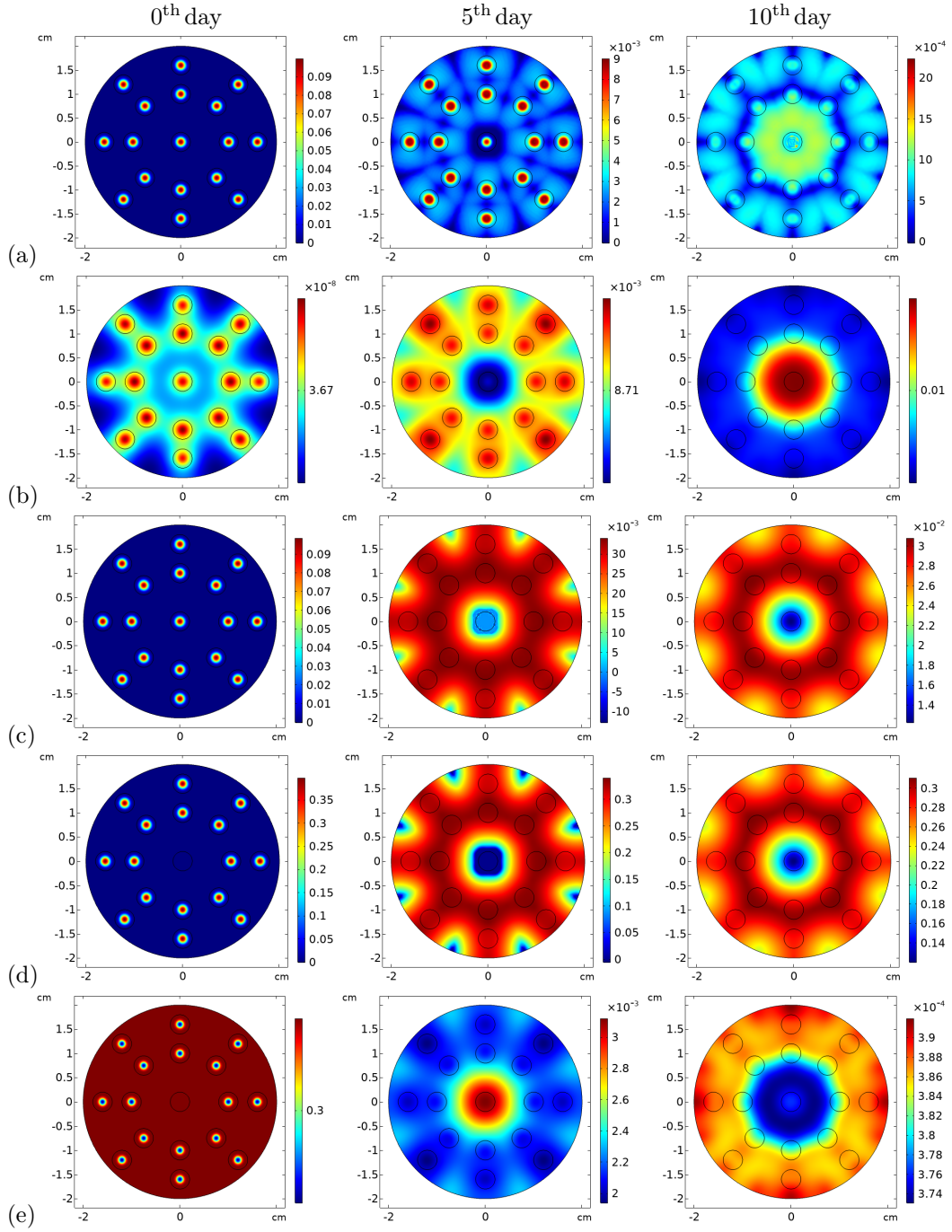**Figure 22.** Geometry and Meshing for the distributed inoculum case.

Figure 23. Surface plots of (a) Active hyphal density, (b) Inactive hyphal density, (c) Hyphal tip density, (d) Internal substrate concentration, and (e) External substrate concentration, on $0^{\text{th}}, 5^{\text{th}},$ and 10th day.
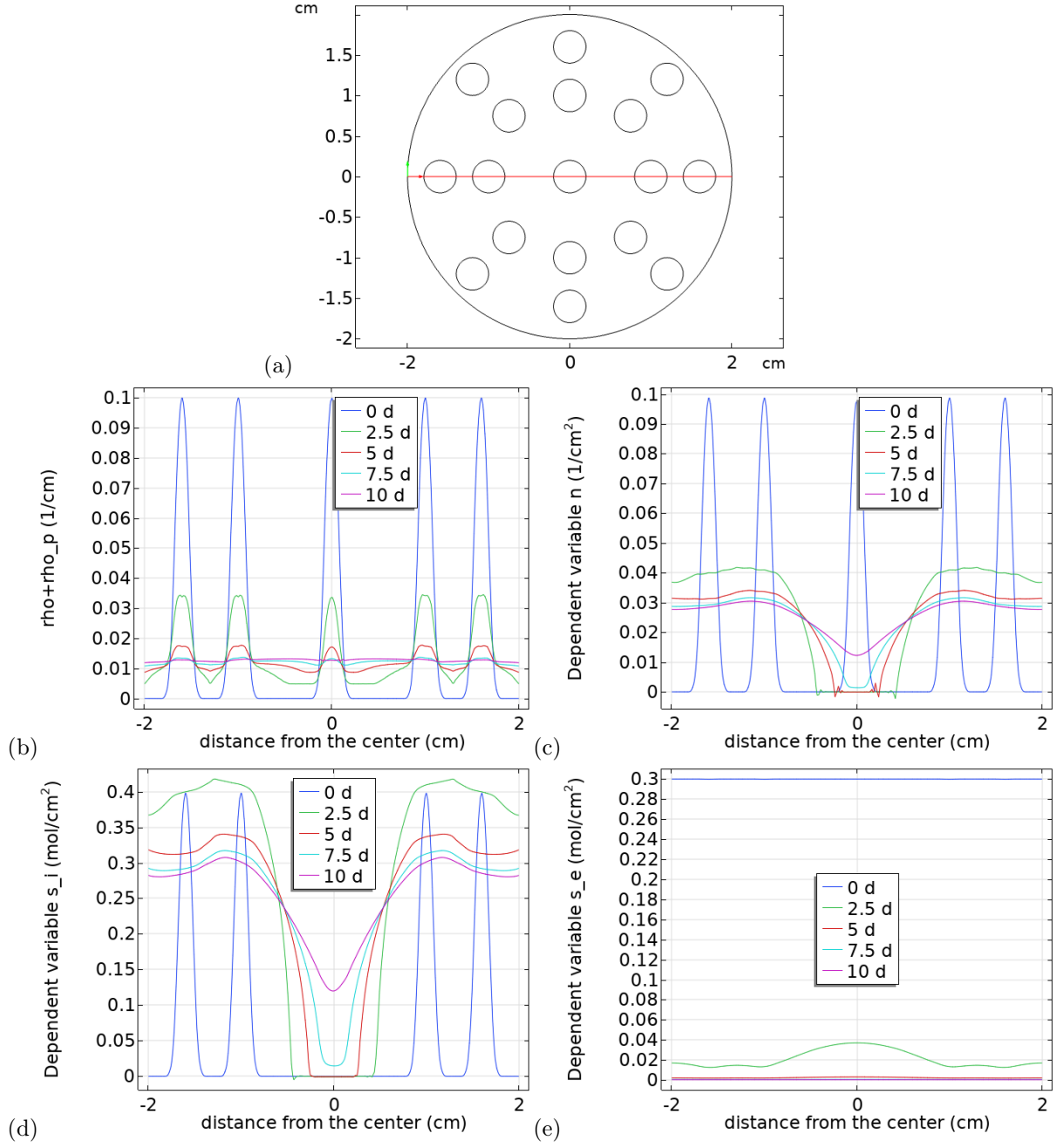
Figure 24. (a) The Cut line along which the line plots of (b) Total hyphal density (active + inactive), (c) Hyphal tip density, (d) Internal substrate concentration, and (e) External substrate concentration, are plotted at different time instants as shown in the legend. $s_{e_{\text{initial}}} = 0.3 \, \text{mol} / \text{cm}^2$

4 Further work

Analysing the distributed inoculum case further by introducing heterogeneity in the external substrate to closely mimic the experimental conditions would be the next step. Solutions from that would be the perfect candidate to test the validity of this model against the experimental observations. Also incorporating the agitation into the equations (as done experimentally in [1]) and possibly obtaining the values of the parameters (Table 1) for *Neurospora Discreta* [1] to match the experiment will also be an avenue to focus on.

Bibliography

[1] R Aravinda Narayanan and Asma Ahmed. Arrested fungal biofilms as low-modulus structural bio-composites: water holds the key. *The European Physical Journal E*, 42(10):1–8, 2019.

[2] Philip Hunter. The mob response: the importance of biofilm research for combating chronic diseases and tackling contamination. *EMBO reports*, 9(4):314–317, 2008.

[3] Emel Ünal Turhan, Zerrin Erginkaya, Mihriban Korukluoğlu, and Gözde Konuray. Beneficial biofilm applications in food and agricultural industry. In *Health and Safety Aspects of Food Processing Technologies*, pages 445–469. Springer, 2019.

[4] Gordon Ramage, Eilidh Mowat, Brian Jones, Craig Williams, and Jose Lopez-Ribot. Our current understanding of fungal biofilms. *Critical reviews in microbiology*, 35(4):340–355, 2009.

[5] Haoyuan Zhou, Yanqing Sheng, Xuefei Zhao, Martin Gross, and Zhiyou Wen. Treatment of acidic sulfate-containing wastewater using revolving algae biofilm reactors: sulfur removal performance and microbial community characterization. *Bioresource technology*, 264:24–34, 2018.

[6] Hans-Curt Flemming and Jost Wingender. The biofilm matrix. *Nature reviews microbiology*, 8(9):623–633, 2010.

[7] Mazza, Marco G . The physics of biofilms—an introduction. *Journal of Physics D: Applied Physics*, 2016.

[8] Michael W Harding, Lyriam LR Marques, Ronald J Howard, and Merle E Olson. Can filamentous fungi form biofilms? *Trends in microbiology*, 17(11):475–480, 2009.

[9] Timothy C Cairns, Xiaomei Zheng, Ping Zheng, Jibin Sun, and Vera Meyer. Moulding the mould: understanding and reprogramming filamentous fungal growth and morphogenesis for next generation cell factories. *Biotechnology for biofuels*, 12(1):1–18, 2019.

[10] Jabed Choudhury. *Mathematical Modelling of Fungal Interactions*. PhD thesis, University of South Wales, 2019.

[11] Maura Harumi Sugai-Guérios, Wellington Balmant, Agenor Furigo, Nadia Krieger, and David Alexander Mitchell. Modeling the growth of filamentous fungi at the particle scale in solid-state fermentation systems. *Filaments in Bioprocesses*, pages 171–221, 2015.

[12] Graeme P Boswell, Helen Jacobs, Fordyce A Davidson, Geoffrey M Gadd, and Karl Ritz. Functional consequences of nutrient translocation in mycelial fungi. *Journal of Theoretical Biology*, 217(4):459–477, 2002.

[13] Graeme P Boswell, Helen Jacobs, Fordyce A Davidson, Geoffrey M Gadd, and Karl Ritz. Growth and function of fungal mycelia in heterogeneous environments. *Bulletin of Mathematical Biology*, 65(3):447–477, 2003.

[14] Graeme P Boswell, Helen Jacobs, Karl Ritz, Geoffrey M Gadd, and Fordyce A Davidson. The development of fungal networks in complex environments. *Bulletin of Mathematical Biology*, 69(2):605–634, 2007.

[15] Karl Ritz and John Crawford. Quantification of the fractal nature of colonies of trichoderma viride. *Mycological Research*, 94(8):1138–1141, 1990.